Review

Addressing Antibiotic Resistance with Bacterial Cytological Profiling: A High-Throughput Method for Antibiotic Discovery

Jhonatan Salgado , James Rayner , Nikola Ojkic *

Posted Date: 29 November 2024

doi: 10.20944/preprints202408.2249.v2

Keywords: antibiotic resistance; bacterial cytological profiling; high-throughput screens; antibiotic mechanism of action; bacterial priority pathogen list; cell segmentation; machine learning; deep learning

Review

Addressing Antibiotic Resistance with Bacterial Cytological Profiling: A High-Throughput Method for Antibiotic Discovery

Jhonatan Salgado, James Rayner and Nikola Ojkic *

School of Biological and Behavioural Sciences, Queen Mary University of London, London, UK
* Correspondence: n.ojkic@qmul.ac.uk

Abstract: Developing new antibiotics poses a significant challenge in the fight against antimicrobial resistance (AMR), a critical global health threat responsible for approximately 5 million deaths annually. Finding new classes of antibiotics that are safe, have acceptable pharmacokinetic properties, and are appropriately active against pathogens is a lengthy and expensive process. Therefore, high-throughput platforms are needed to screen large libraries of synthetic and natural compounds. In this review, we present bacterial cytological profiling (BCP) as a rapid, scalable, and cost-effective method for identifying the mechanisms of action of antibiotics offering a promising tool for combating AMR and drug discovery. We present the application of BCP for different bacterial organisms and different classes of antibiotics and discuss BCP's advantages, limitations, and potential improvements. Furthermore, we highlight the studies that have utilized BCP to investigate pathogens listed in the Bacterial Priority Pathogens List 2024 and we identify the pathogens whose cytological profiles are missing. Lastly, we explore the most recent artificial intelligence and deep learning techniques that could enhance the analysis of data generated by BCP, potentially advancing our understanding of antibiotic resistance mechanisms and the discovery of novel druggable pathways.

Keywords: antibiotic resistance; bacterial cytological profiling; high-throughput screens; antibiotic mechanism of action; bacterial priority pathogen list; cell segmentation; machine learning; deep learning

1. Introduction

The World Health Organization (WHO) has declared antimicrobial resistance (AMR) as one of the most severe global health threats facing humanity. AMR is the ability of a microbe to survive and grow in the presence of a chemical thought to prevent this effectively. It has been estimated that in 2019 alone, antimicrobial resistance killed at least 1.27 million people globally, more deaths than HIV/AIDS or malaria, with 4.95 million deaths associated with AMR[1]. According to the Centers for Disease Control and Prevention's Antibiotic Resistance Threats Report[2], in the United States, over 2.8 million antibiotic-resistant infections appear every year, leading to over 35,000 deaths. Furthermore, AMR has been predicted to lead to a total loss of up to $100 trillion for the global economy by 2050[3]. These alarming statistics underscore the urgent need to develop effective therapeutics to combat antimicrobial resistance.

The efforts undertaken in the field of AMR until now have not been enough despite the enormous research effort and inventive therapeutic approaches. Since 1940, antimicrobials have been used widely[4],[5] and beyond treating infections, antibiotics enabled many modern medical procedures, such as open-heart surgeries, organ transplants, and cancer therapies[6]. Even before 1940 and for about 60 years after, most antibiotics were discovered by culturing microbial samples from soil for compounds already expressed by microbes[7],[6]. However, over the last 20 years, the lipopeptides and the oxazolidinones have been the only two new antibiotic classes created and have been effective only against Gram-positive bacteria[8]. The last novel antibiotic class introduced to kill Gram-negative bacteria was the quinolones when nalidixic acid was synthesized in 1962[9]. Although recent developments have shown potential against Gram-negative bacteria, such as Zosurabalpin, a

 doi:10.20944/preprints202408.2249.v2

new antibiotic that disrupts bacterial lipopolysaccharide (LPS) transport from the inner membrane to the outer membrane[10], further advancements in antibiotic discovery are needed. To facilitate the discovery of novel druggable pathways, new high-throughput screens based on Bacterial Cytological Profiling have been developed.

This review emphasizes the use of bacterial cytological profiling (BCP) as a highly effective method for discovering novel antibiotics and rapidly identifying antibiotic targets in a cost-effective manner. BCP initially creates a library that captures the overall profile of bacterial morphological and physiological changes at a single-cell level induced by antibiotics with known mechanisms of action. This profile includes details on bacterial cell shapes and sizes, fluorescent intensities and spatial distribution of DNA, and fluorescent distribution of membrane dyes[11–13]. The library is then utilized to classify existing antibiotics based on the specific components of bacterial cells they target and to discover new antibiotics. In this review, we also highlight how BCP is used to expand our quantitative understanding of antibiotic pharmacodynamics and bacterial stress responses, as well as how BCP enhances the development of non-traditional antibacterial strategies such as phage therapies[14–20].

2. Antibiotic Mechanism of Action and Antibiotic Targets

AMR arises from either genetic alterations or phenotypic changes in pathogens[21,22]. To effectively tackle antibiotic-resistant bacteria, it is essential to understand how antibiotics work, which is known as their mechanism of action (MOA), see Table 1. Understanding MOA involves studying how antibiotics affect bacterial physiology and molecular interaction with bacterial targets (Figure 1). However, identifying the MOA presents a significant limitation in drug discovery.

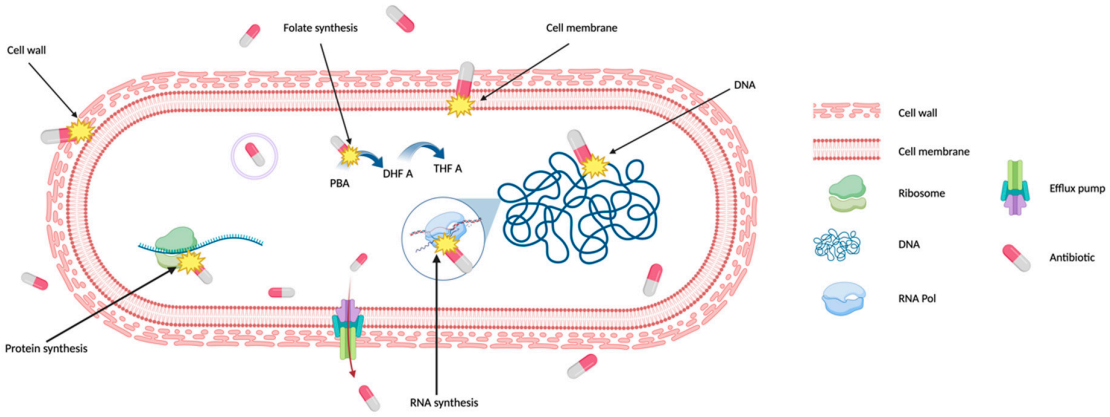

Figure 1. Antibiotic targets in bacteria. Antibiotics typically kill bacteria by targeting at least one of the five cell components: cell wall, cell membrane, ribosomes, DNA, and RNA. Antibiotics interfere with the synthesis or directly damage of cell structures to inhibit bacterial growth or irreversible damage bacterial integrity. Some antibiotics inhibit the synthesis of essential cell components, such as folate synthesis, a precursor for DNA synthesis. Figure is created using BioRender. .

Traditionally, the pathway inhibited by a compound has been identified mainly through macromolecular synthesis (MMS) assays. These assays use radioactively labelled precursors for peptidoglycan, lipid, protein, RNA, or DNA synthesis[23], therefore enabling the identification of whether one or more pathways are targeted. Despite being an important technique, MMS assays are limited by low accuracy, low resolution, low throughput and time-consuming[13].

Table 1. *General classification of antibiotics based on their target and chemical structure, including their mechanism of action. Examples of each antibiotic type are included.

 doi:10.20944/preprints202408.2249.v2

Target	*Chemical Structure*	*Mechanism Of Action*	*Generic Name Examples*
Cell Wall	b-Lactams	Inhibit penicillin-binding proteins (PBPs) that crosslink peptidoglycan chains in the bacterial cell wall[24], disrupting cell wall integrity and causing cell lysis[25].	Penicillins, cephalosporins, cephamycins, carbapenems, and others.
	Glycopeptides	Bind to the acyl-D-Ala-D-Ala terminus of peptidoglycan in Gram-positive bacteria[26].	Vancomicyn
Membane	Lipopeptides	Depolarize the cell membrane, reducing the ability to create ATP and inducing cell death[27].	Daptomycin, Colistin
Fatty Acid Synthesis	Chlorophenol	Inhibit *fabI*, an enoyl-ACP reductase, blocking the fatty acid synthesis[28].	Triclosan
	Oxirane carboxylic acids	Bind to b-ketoacyl-acyl carrier protein synthase, inhibiting fatty acid synthesis. In sterol synthesis, inhibits HMG-CoA synthetase activity[29].	Cerulenin
Protein Synthesis	Aminoglycosides	Cause mRNA misreading and production of uncompleted proteins by targeting the 30s ribosomal subunit of 16S RNA resulting in cell death[25]. [30].	Gentamicin, tobramicin, kanamycin
	Tetracyclines	Bind to 16S rRNA of the 30S ribosomal subunit, inhibiting tRNA binding to 30S and preventing translation[31].	Tetracycline, doxycycline and lymecycline
	Macrolides	Bind to the 23S rRNA of the 50S ribosomal subunit, leading to incomplete peptide chains[32].	Azithromicin, erythromycin and clarithromicyn
	Lincosamides	Bind to the 50S ribosome subunit, causing the peptidyl-tRNA molecule to detach from the ribosome during elongation[33].	Clindamicyn
	Oxazolidinones	Inhibit the correct 70S ribosome subunit formation by binding to the 23S rRNA of the 50S subunit[34].	Linezolid
DNA Synthesis	Fluoroquinoles	Target DNA gyrase and topoisomerase IV inhibiting DNA replication[35,36].	Ciprofloxacin and levofloxacin
	Sulfonamides	Competitive inhibitor of Dihydropteroate synthase (DHPS) involved in folate synthesis[37].	Sulfamethazine, sulfapyridine
RNA Synthesis	Rifamycins	Bind to the RNA polymerase and block the RNA synthesis[38].	Rifapentine, Rifampin

*For more detailed classifications based on the antibiotic targets see [[28,37,38]] or classifications based on chemical structure, see [[39]].

 doi:10.20944/preprints202408.2249.v2

To address the limitations associated with MMS assays, diverse alternative techniques for determining the MOA have been developed[40]. These include biochemical approaches, such as affinity chromatography, which identifies direct biophysical interactions between antimicrobials and their targets where the antibiotic interacts with protein from whole-cell extracts[41–43]. Genetic approaches, such as selection for resistance and resistance screening[41], focus on the genetic comparison between non-resistant strains and strains that have evolved and mutated to become resistant to a specific antibiotic.

While these additional methods offer several benefits, they also have limitations that influence their effectiveness. The primary challenge is the required time to conduct the assays. Additionally, these methods require large amounts of purified compounds, which can be difficult to obtain, especially since newly discovered compounds are usually available in limited amounts[13]. Apart from all limitations in determining MOA, discovering novel compounds that are active against Gram-positive and Gram-negative bacteria remains challenging.

The process of discovering and developing new classes of antibiotics is particularly challenging, as they must exhibit acceptable pharmacokinetic properties, demonstrate safety, and efficacy[9]. Moreover, producing antibiotics offers limited profit margins due to the high production costs and the extended process of research, testing, and approval[9]. Therefore, new, high-throughput screening platforms are needed for the fast and inexpensive screening of large libraries of synthetic and natural compounds that are highly effective against human pathogens[44,45]. The following section reviews the quick and scalable bacterial cytological profiling methods (BCPs) and discusses their availability for some of the most important human pathogens as outlined in the latest WHO 2024 report.

3. BCP to Identify the Mechanism of Action

In 2013, Poochit *et al.* designed Bacterial Cytological Profiling (BCP) analysis for *E. coli* cells using different classes of antibiotics[13] (Figure 2). BCP data are obtained using fluorescent microscopy of *E. coli* cells stained with fluorescent membrane and DNA dyes as well as fluorescent reporter for membrane permeability. Using image analysis software, various bacterial cell parameters, such as cell length, width, solidity, and DNA content, are extracted[13]. Subsequently, complex multidimensional data are analyzed using the *Principal Component Analysis (PCA)* technique, to cluster cells based on their cytological profile to identify the MOA of known and unknown antibacterial compounds (Figure 2B, Box 1). Since cytological profiling produces data at a single-cell level[12], it uses morphological data such as bacterial chromosomal condensation, or cell shape changes in response to antimicrobials to differentiate between different targeted metabolic pathways [13] (Figure 2B). Furthermore, this approach can lead to the identification of antibiotics that are effective against multidrug-resistant bacteria[11].

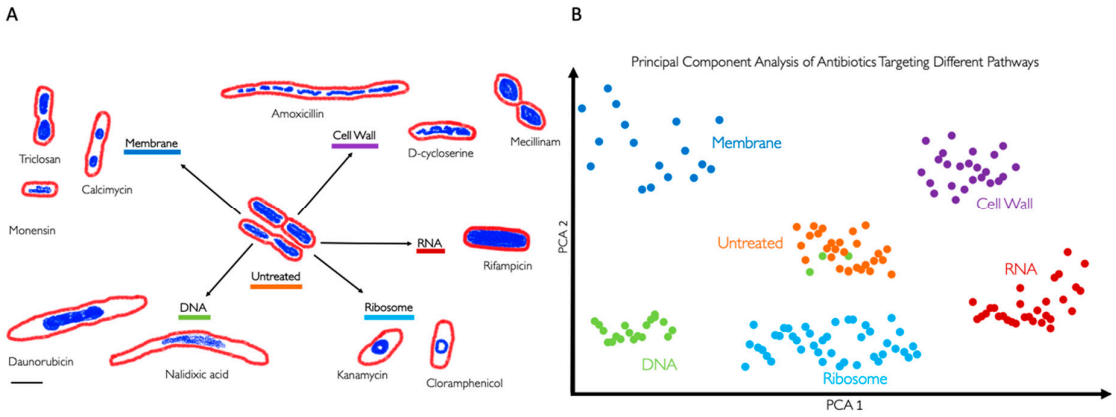

Figure 2. **Bacterial Cytological Profiling. (A)** Antibiotics that target different bacterial cell components induce different cell morphologies. The drawings are based on the microscopy images

 doi:10.20944/preprints202408.2249.v2

from Poochit et al.[13], where bacterial cells were treated with antibiotics targeting five major biosynthetic pathways (DNA, Ribosome, RNA, Cell Wall, Membrane), using fluorescent dyes FM4-64 (red) and DAPI (blue) to stain bacterial membranes and DNA respectively. Scale bar, 1 μm. **(B)** Principal Component Analysis (PCA) is used to cluster different bacterial cell shapes based on the antibiotic MOA. Each point on the graph represents a single cell. The graph also illustrates that when green dots, representing a characteristic morphology of a DNA-targeting antibiotic, cluster with orange dots, representing untreated bacteria, indicating no morphological change and suggests possible antibiotic resistance or persistence[46,47].

Box 1. Principle Component Analysis (PCA).

PCA is a popular statistical technique commonly used for identifying linear relationships in complex data by identifying the fewest variables which contribute the most to variance in the data[48]. PCA creates a linear combination of the original variables to create a new set of principal components[48]. Firstly, PCA starts by calculating a matrix showing the relation each variable has for all others. Then, it finds their eigenvectors (direction of the relationship) and eigenvalues (contribution of relationship to variance). In PCA, the principal components with the most contribution to variance in the data are then plotted. PCA has diverse applications across almost all scientific fields, including biology, medicine, computer science, and geology. In the context of biomedical research, PCA has been utilized to analyze the human cell atlas and prostate cancer risk prediction[49,50]. Whilst PCA captures linear relationships between variables exclusively, it has been the primary method for dimensional reduction in Bacterial Cytological Profiling (Fig. 2B). There are also recent popular approaches capturing non-linear relationships such as UMAP[51] (primarily local differences), or PaCMAP[52] (local and global relationships) which may provide other insights into local differences and non-linear relationships within and between antibiotic treatments. Additionally, plots of dimensionally reduced provide insightful comparisons between different treatments, however, identifying distinct profiles is not equivalent to identifying novel targets; a drug could have multiple known MOAs for example and still display a distinct profile[12,53]. Even so, there have been possible connections found between various BCP profiles and novel targets using PaCMAP[54].

BCP takes advantage of the limited presence of cell-cycle checkpoints in bacteria[13]. When stressed by antibiotics, bacteria show phenotypical changes that are characteristic of the antibiotic target. For example, compounds that target the ribosome by stopping protein synthesis (e.g., tetracycline and chloramphenicol) produce circular chromosomes and wide cells[13,55] (**Error! Reference source not found.**).

During antibacterial treatment, rod-shaped bacteria (bacilli) can shrink and take on an oval form, known as ovoid cells[56,57]. There are no clearly defined names for these cells, however, as they have been referred to in literature as 'round forms'[58,59]; 'round cells'[60–62]; 'spherical forms'; 'spherical cells'[63–65]; or 'coccoid forms'[66,67]. Filamentation, or cell elongation, occurs when rod-shaped bacteria (or sometimes cocci) synthesize peptidoglycan for their side walls but not for their division walls, leading to abnormally elongated cells[68]. This process results from the inhibition of septal peptidoglycan synthesis[56]. Filamentous cells can be also induced when DNA synthesis is inhibited[69,70] or DNA is damaged[71–73] by a process known as the SOS response that inhibits cell division [36](Fig. 2).

Antibiotic treatments can drastically alter bacterial cell size, induce localized swelling, bulge formation, blebbing, and thicken peptidoglycan[68]. Occasionally, antibiotic-treated cells can lose cell walls, turning bacterial cells into spheroplasts and protoplasts. Spheroplast are Gram-negative bacteria that lost their peptidoglycan layer, but kept their outer membrane, whereas protoplasts are

 doi:10.20944/preprints202408.2249.v2

formed from Gram-positive bacteria that lack the peptidoglycan layer[74]. Bacterial variants that completely lack a cell wall, encompassing both Gram-negative and Gram-positive bacteria, are also known as *L-forms*[75–78].

Phenotypical changes could confer an increase in fitness to bacteria in the presence of antibiotics[79]. Resistance to antibiotics usually takes the form of reducing the concentration of intracellular antibiotic or by reducing the binding affinities of the cellular targets to the antibiotic[80]. By using available BCP data, recent studies have shown that by reducing the surface-to-volume ratio (*S*/*V*), bacteria can effectively reduce the antibiotic concentration inside a cell, thereby promoting cell growth by decreasing antibiotic influx[80]. Similarly, an increase in *S*/*V* can benefit the cell in alternative ways such as increasing the antibiotic efflux rate or the rate of nutrient uptake[80–82]. These studies explain how cell shape transformations promote bacterial survival under antibiotic treatments – pointing towards potential new druggable targets that control cell shape and size under stress.

BCP has been successfully employed to study the MOA of various antibacterial agents, including azithromycin[83], diphenylureas[84] and thailandamide[85]. It has also been used to identify the cellular pathways targeted by anticancer metal complexes[86] and to study the response of bacteria to antibiotics in different growth conditions[87]. Additionally, BCP has been used to identify the cellular pathways targeted by antibacterial molecules affecting different cellular pathways[88],[89], making it a valuable tool not only for determining antibacterial targets but also to potentially identify novel MOA i.e., ones that target new proteins or new pathways (Figure 3).

BCP can also be used to determine the MOA of treatments beyond antibiotics, such as phage therapies, revealing how phages disrupt essential cellular pathways[14–20]. BCP allows the visualization of bacterial chromosomal condensation, cell shape and overall cellular morphology changes within bacterial cells during phage infection. These changes not only reveal the pathways and cellular targets phages use to propagate their lifecycle but also highlight the role of bacterial defense mechanisms in combating phage infection[15,17,20]. BCP has demonstrated how the overexpression of phage-related proteins can induce specific phenotypic changes as a result of the activation of a bacterial defense system to suppress phage propagation[14]. Additionally, BCP has been fundamental in assessing the impact of different antibiotics on phage replication, revealing that certain antibiotics can synergize with phages to enhance bacterial cell lysis. In contrast, others inhibit phage propagation by disrupting essential bacterial processes[15]. This dual capability of BCP to show both the direct effects of phage infection and the influence of external agents such as antibiotics, makes it a high-throughput tool in studying phage-bacteria dynamics.

4. BCP of Important Human Pathogens

Most importantly, BCP has been successfully used to study some of the most important human pathogens from the WHO Bacterial Priority Pathogens List (Table 2). In 2017, the first Bacterial Priority Pathogen list was created by the WHO in collaboration with researchers from the Division of Infectious Diseases at the University of Tübingen, Germany which used a multicriteria analysis technique to inform research and development (R&D) for future antibacterial compounds[90]. Now, seven years after the introduction of the list there have been novel antibiotics put onto the market either with effectiveness *in vivo* or *in vitro* against pathogens deemed critical priority, but unfortunately, resistance has been found in almost every one[91,92]. This year the WHO updated this list to tackle new developments in antimicrobial resistance to give an updated and directions for policy makers and insight on future developments. The new Bacterial Priority Pathogens List 2024 includes 15 resistant pathogens, ordered at various levels of priority from medium; high; to critical[93] (Table 2). Out of 15 pathogen groups, bacterial cytological profiling is not available for 30 % of them: *Non-typhoidal Salmonella, Neisseria gonorrhoeae,* Group A and B *Streptococci, Haemophilus influenzae*. Therefore, urgent BCPs regarding these severe pathogenic organisms are needed.

 doi:10.20944/preprints202408.2249.v2

Table 2. BCP Analysis for the WHO Bacterial Priority Pathogens List (2024). In third column, this table indicates whether bacterial have been studied using Bacterial Cytological Profiling (BCP) or not. We consider any BCP done in wild-type strains rather than AMR pathogen strains.

Bacteria	Resistant to	Bacterial Cytological Profilling (BCP)
Priority 1. Critical group		
Acinetobacter baumannii	Carbapenems	Yes[12,83,94]
*Enterobacteriaceae**	Third generation cephalosporine	Yes[13,86,95–97]
*Enterobacteriaceae***	Carbapenems, ESBL-producing	Yes[83,98,99]
*Rifampicin-Resistant Tuberculosis (RR-TB)****	Rifampicin	Yes[100,101]
Priority 2. High group		
Salmonella Thypi	Fluoroquinolones	Yes[99]
Shigella spp.	Fluoroquinolones	Yes[102]
Enterococcus faecium	Vancomycin	Yes[103]
Pseudomonas aeruginosa	Carbapenems	Yes[15,83,98,99]
Non-typhoidal Salmonella	Fluoroquinoles	No
Neisseria gonorrhoeae	Cephalosporin, Fluoroquinolonas	No
Staphylococcus aureus	Methicillin and vancomycin	Yes[11,84,104,105]
Priority 3. Medium group		
Group A *Streptococci*	Macrolide	No
Streptococcus pneumoniae	Macrolide/No sensitivity to penicillin	Yes[106]
Haemophilus influenzae	Ampicillin	No
Group B Streptococci	Penicillin	No

* The BCP column uses *Escherichia coli* as a reference for this group. ** The BCP column uses *Klebsiella pneumoniae* as a reference for this group. ***RR-TB was evaluated independently in a tailored approach so it was technically "not" included in the list but after the evaluation by specialists, it was determined as a critically dangerous bacteria therefore. RR-TB stands apart from the list due to the distinct nature of its evaluation process.

5. BCP to Identify New Druggable Cell Pathways

BCP is used to scan new antibacterial components to identify their specific targets (Fig. 3). As demonstrated, BCP effectively differentiates between various morphological changes induced by different antibiotics, thereby providing insights into the antibiotic's MOA. If a novel antibiotic places bacteria in a distinct region of the PCA plot compared to known antibiotic targets, it could indicate a new pathway target or MOA previously uncharacterized (Fig. 3). For example, if the PCA analysis shows that the morphology of bacteria treated with a new antibiotic clusters in a region associated with membrane or RNA targets (Arrows 2 and 3 in **Error! Reference source not found.**), it directly indicates the antibiotic's mode of action. Conversely, if the antibiotic's effect causes a morphology

 doi:10.20944/preprints202408.2249.v2

change that places bacteria in a novel zone, as illustrated with Arrow 4, it may suggest the discovery of a new antibacterial pathway or target.

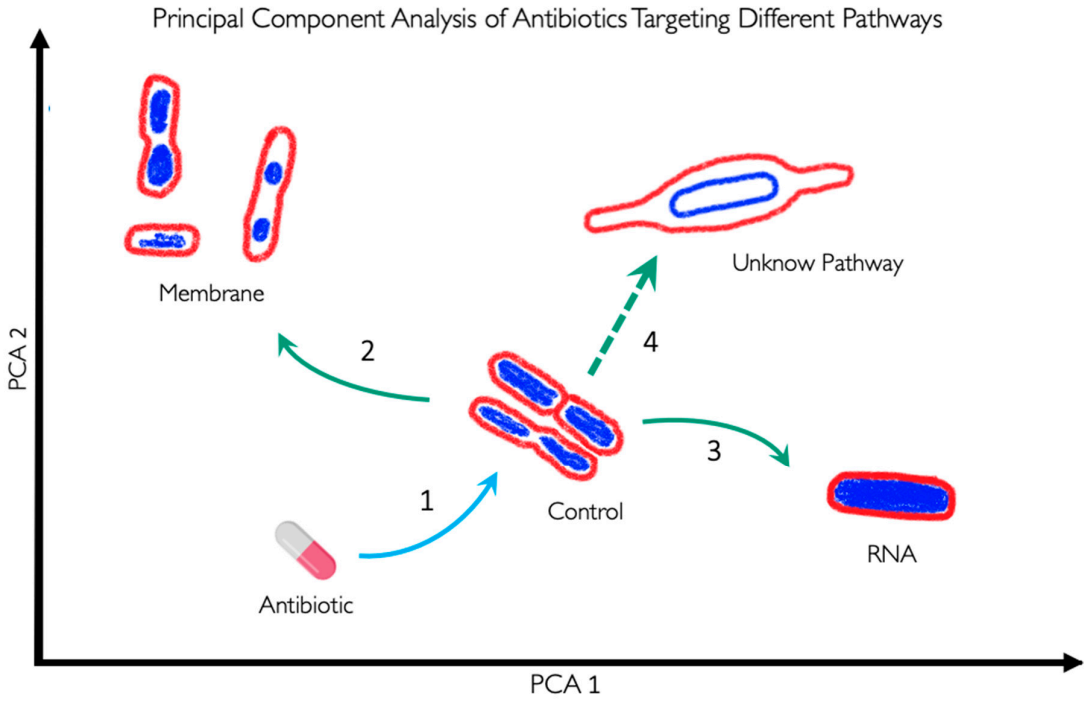

Figure 3. Representation of Principal Component Analysis (PCA) using bacterial morphologies to determine the MOA of a novel antibiotic. Arrow 1 indicates the antibiotic used against certain bacteria, which can change their shape depending on the antibiotic's MOA. If the bacteria exhibit a morphology as indicated by arrow 2, the antibiotic targets the membrane. Conversely, if the bacteria display a morphology as indicated by arrow 3, the antibiotic targets RNA. However, if the morphology is completely different from the known and clustered morphologies, as shown by arrow 4, it suggests that the antibiotic targets a novel pathway and if the bacteria do not show any change, it suggests that they are not susceptible to this antibiotic or, in the worst-case scenario, that they are resistant to the antibiotic.

Together, BCP significantly enhances drug development by offering a precise, fast and systematic method for characterizing the effects of new antibacterial agents. Its ability to identify target-specific morphological changes provides a comprehensive tool for uncovering novel antibiotic targets and advancing our understanding of bacterial physiology.

6. BCP Limitations

Even with all the advantages we mentioned about BCP, it has certain limitations. BCP can identify the general target of an antibiotic, but it cannot provide precise information about the exact site within the target that is affected. For instance, while BCP can indicate that an antibiotic targets the ribosome, it cannot specify which part of the ribosome is involved.

BCP requires staining dyes to evaluate DNA content and cell size and shape, with fluorescent dye intensity being essential for determining the antibiotic MOA. A wide variety of dyes, protein fusions, and reporter strains have been used in BCP, facilitating both fast MOA detection, and discovery of new MOAs. However, despite the abundance of possible dyes, strains, and assays selecting the most appropriate ones for specific phenotypic experiments remains challenging, as more information is needed to understand cellular functions (**Error! Reference source not found.**). This is exacerbated by the complexity of bacterial physiology with many processes being overlapped by mechanisms such as metabolic flux or co-dependent regulation [107]·[108].

 doi:10.20944/preprints202408.2249.v2

Table 3. Studies with bacterial profiles following the original BCP method. This table includes the organisms studied, the dyes used to visualize cellular components, data availability, and image analysis methods used to extract data for profiling.

Organism	Dyes/Fluorophores	Processed Data available	Segmentation	Feature extraction	Source
Acinetobacter baumannii and *E. coli*	FM4-64 DAPI SYTOX-Green	Yes	CellProfiler[109]	CellProfiler[109]	[94]
Acinetobacter baumannii	FM4-64 DAPI SYTOX-Green	No	Ilastic[110]	CellProfiler[109]	[12]*
Pseudomonas aeruginosa	FM4-64 DAPI	Yes	Manually (FIJI/ImageJ[111])	Manually (FIJI/ImageJ[111])	[15]*
S. aureus	FM4-64 DAPI SYTOX-Green	Yes	Semi-Manual (FIJI/ImageJ[111])	Semi-Manual (FIJI/ImageJ[111])	[13]*
S. aureus	FM4-64 DAPI SYTOX-Green WGA-647	Yes	CellProfiler[109]	CellProfiler[109]	[11]*
S. aureus, *S. Typhimurium*, and *K. pneumoniae*	FM4-64 DAPI SYTOX-Green	Yes	Harmony[112]	Harmony[112]	[99]
B. subtilis	FM 4-64 DAPI SYTOX Green	Yes	CellProfiler[109]	CellProfiler[109] FIJI	[113]*
B. subtilis	FM4-64 DAPI SYTOX-Green	No	CellProfiler[109]	CellProfiler[109]	[114]*
B. subtilis	Nile red DAPI	No	MicrobeJ[115]	MicrobeJ[115]	[107]*
Bacillus subtilis, *E. coli*	FM4-64 DAPI GFP	No	Wasabi software (Hamamatsu)	Wasabi software (Hamamatsu)	[88]
E. coli	FM4-64 Hoechst-33342 Dendra2 protein	No	FIJI/ImageJ[111]	FIJI/ImageJ[111]	[86]
E. coli	FM4-64 DAPI SYTOX-Green	No	Semi-Manual (FIJI/ImageJ[111])	Semi-Manual (FIJI/ImageJ[111])	[116]*

 doi:10.20944/preprints202408.2249.v2

M. tuberculosis Erdman	FM4-64FX SYTO 24	Yes	MorphEUS[117]	MorphEUS[117]	[100]*

*Pipelines, scripts, or instructions are detailed and/or included in the paper. Programs are also widely accessible.

Table 4. Studies using protocols similar to the original BCP method. This table includes the organisms studied, the dyes used to visualize cellular components, whether the data is available online, and image analysis methods used to extract data for profiling.

Organism	Dyes/Fluorophores	Processed Data available	Segmentation	Feature extraction	Source
E. coli *Caulobacter crescentus*	FM4-64 DAPI	No	Oufti[118]	Oufti[118]	[119]*
Achromobacter xylosoxidans	FM4-64 DAPI SYTOX-Green NBD Azithromycin	No	FIJI/ImageJ[111] and CellProfiler[109]	FIJI/ImageJ[111] and CellProfiler[109]	[120]
M. smegmatis	ParB-mCherry	Yes	MicrobeJ[115]	MicrobeJ[115]	[121]*
Shewanella putrefaciens	Ffh-mVenus FtsY-mVenus uL1-mVenus	Yes	FIJI/ImageJ[111]	FIJI/ImageJ[111]	[122]*
V. parahaemolyticus	FM4-64 DAPI	No	FIJI/ImageJ[111]	FIJI/ImageJ[111]	[18]
Bacillus subtilis	FM4-64 DAPI SYTOX-Green SYTO-9	No	-	Manual w/ FIJI[111]	[123]*
M. smegmatis *M. tuberculosis*	FM4-64 GFP CellROX	Yes	Omnipose[124]	Manual w/ FIJI or with Cell Counter installation in FIJI Custom python script	[125]
E. coli *B. subtilis*	FM4-64 DAPI GFP DiSC	No	FIJI/ImageJ[111] and MicrobeJ[115]	FIJI/ImageJ[111] and MicrobeJ[115]	[126]
E. coli *S. aureus* *Bacillus subtilis*	Nile Red DAPI mScarlet	Yes	StarDist[127] CARE[128] pix2pix[129] ML-U-Net[130] SplineDist[131]	Classification without feature extraction, using Deep Learning	[132]

 doi:10.20944/preprints202408.2249.v2

*Pipelines, scripts, or instructions are detailed and/or included in the paper. Programs are also widely accessible.

7. BCP Potential Improvements

As shown in **Error! Reference source not found.** and 4, a variety of fluorescent dyes have been used to investigate the cytological profiles of different bacterial organisms. However, newly developed dyes have the potential to provide more detailed information that could help in building a more comprehensive response profile. Despite the prevalence of cell wall targeting antibiotics in BCP experiments, direct methods for visualizing cell wall synthesis and remodeling during antibiotic exposure have been lacking. In 2012, Kuru *et al.* discovered a groundbreaking method for bacterial cell wall staining using fluorescent amino acids[133]. The cell wall provides the shape and structural integrity of the cell. It is made of peptidoglycan (PG), which consists of glycan strands cross-linked by D-amino acid (DAA)[134]. The team introduced HADA and NADA, two fluorescent D-amino acids (FDAAs) attached to a D-amino acid backbone (3-amino-d-alanine). This chemical biology approach aims to detect and visualize the exact location and amount of new peptidoglycan layer synthesis in bacteria. By using HADA or NADA as a fluorescent peptidoglycan label during cell wall synthesis, the technique also allows researchers to observe morphological changes in bacteria over time. This is relevant as HADA and NADA can be implemented in the methodology of BCP to investigate the growth modes of bacteria under antibiotic exposure as they exhibit a diverse growth pattern – that could confer selective advantages in their environments[135]·[80].

Other fluorescent dyes are available to quantitatively probe bacterial physiological states: ThT and $DiBAC_4$ for bacterial membrane potential[136–139], carboxy-H_2DCFDA for reactive oxygen species (ROS)[139], and DAF-FM for reactive nitrogen species (RNS)[139]. By integrating membrane potential, ROS, and RNS into cytological profiles could provide additional information regarding bacterial physiology and bacterial stress response during antibiotic treatment.

8. Image Analysis Tools for BCP and Data Availability

Fluorescent microscopy has allowed us to visualize many cell components in great clarity, however, quantitative image analysis of both cellular and sub-cellular structures has been a continual challenge[125,140]. The requirement for accurate tools is highlighted by the scale of the bacterial objects, with typically 100-300 pixels per typical *E. coli* cell[124], while antibiotic-treated cells could have an order of magnitude larger sizes[13]. In addition to variations in size, bacteria exhibit a diverse array of shapes[135]. While most studied bacteria in BCP (see Table 3 and 4) are rod-shaped or spheroid, there is growing interest in bacteria with more complex shapes that emerge after exposure to antibiotics, such as seen in *Caulobacter crescentus*[79].

To precisely define cell boundaries and to segment cellular components, sub-pixel segmentation methods are required[124],[141]. Many segmentation solutions are currently available as user-friendly plugins such as MicrobeJ (using classical segmentation), within easily accessible platforms such as ImageJ[140,142,143]. Stand-alone image analysis programs are also available but these can at times be less supported and less accessible[118]. Classical image segmentation techniques have been used since the 1960s[144,145], laying the groundwork for the more advanced artificial intelligence methods used nowadays.

In 2016 SuperSegger was created to improve upon flaws in segmentation through thresholding in bacterial phase-contrast images and it combines classical segmentation with Deep learning[146]. To correct common errors in segmentation from both the thresholding and watershed, SuperSegger uses a shallow neural network trained from the segmentation data[147]. Recently, Deep neural networks (DNNs) which have now become the backbone of most Deep learning segmentation methods are now widely recognized as superior tools for cell segmentation[148]. As showcased in Table 3, Deep learning is significantly underutilized in original BCP studies. However, some recent BCP profiles have been created using Deep learning for segmentation and object detection (Table 4).

Among recent and easily available Deep learning segmentation algorithms, Pachitariu *et al.* demonstrated that Cellpose outperformed the popular programs Mask R-CNN and StarDist when applied to a varied dataset of different cell types and cell-like-objects, showcasing it as a powerful

 doi:10.20944/preprints202408.2249.v2

general solution for cell segmentation[142]. Cutler *et al.* assessed the performance of (at the time) state-of-the-art cell segmentation algorithms on a wide array of bioimages of bacteria with different morphologies. This led to the design of the algorithm, *Omnipose*, which outperforms all segmentation algorithms tested across a varied dataset of bacterial cell sizes, shapes, and optical characteristics and as such has been used extensively in research[124]. Beyond segmentation, Deep learning has been used to predict morphologies of unlabeled cells, allowing researchers to simulate more tags than are currently possible to image at once and potentially extending the power of cytological profiling[149,150].

Segmented data availability (Table 3 and 4) is invaluable for scientific communities and accelerates new findings. By using published BCP data and mathematical modelling, the researchers uncovered the robustness of scaling behavior between cell surface area and volume in *E. coli*[81] and *B. subtilis*[82], inferred cell physiological alterations upon antibiotic treatments[151], and proposed a new antibiotic resistance pathway mediated by cell surface-to-volume ratio (*S/V)* transformations[80]. Therefore, the availability of BCP data is good practice and should be considered as a benchmark for all future BCP platforms, especially for pathogenic bacteria (Table 2).

9. Conclusions

Despite significant advances in research and the development of new tools, combating antimicrobial resistance (AMR) requires a multifaceted approach. Continued investment in research and development, global collaboration, and the effective implementation of surveillance and prevention strategies are crucial. Bacterial Cytological Profiling (BCP) stands out as a rapid and cost-effective technique that facilitates drug discovery by revealing the mechanism of action of novel antibacterial agents through detailed physiological and morphological analysis. Furthermore, BCP could be used to identify phenotypic changes when multiple antibiotics are used, revealing unique or overlapping cell morphologies induced by these combinations[12]. However, systematic explorations of cytological profiles for drug combinations are still missing.

Apart from bacteria, cytological profiling methods are also widely used for other organisms such as yeast[152,153], fungi[154], and human cells[155–157]. Deep learning techniques employed for yeast and human cells have been used without feature extraction, however, this method has not yet been applied to bacteria. Therefore, wider availability, applications and integration of machine learning tools across different scientific fields are needed.

Besides BCP being used to discover new antibiotics, BCP has been used to investigate complex interactions between bacteria and their predators – bacteriophages[14–16]. BCP enables the identification of metabolic pathways and cellular processes targeted by phages and antibiotics, both individually and in combination. Therefore, BCP reveals molecular mechanisms governing the phage-bacteria interaction, ultimately paving the way for more effective phage-based antibacterial therapies.

Acknowledgments: We gratefully acknowledge funding from BBSRC (BB/Y009002/1).

References

1. Murray, C.J.L.; Ikuta, K.S.; Sharara, F.; Swetschinski, L.; Robles Aguilar, G.; Gray, A.; Han, C.; Bisignano, C.; Rao, P.; Wool, E.; et al. Global burden of bacterial antimicrobial resistance in 2019: a systematic analysis. *The Lancet* **2022**, *399*, 629–655, doi:10.1016/S0140-6736(21)02724-0.
2. Centers for Disease Control and Prevention (U.S.) *Antibiotic resistance threats in the United States, 2019*; Centers for Disease Control and Prevention (U.S.), 2019;
3. O'Neill, J. Tackling drug-resistant infections globally: final report and recommendations. **2016**.
4. GARDNER, A.D. Morphological Effects of Penicillin on Bacteria. *Nature* **1940**, *146*, 837–838, doi:10.1038/146837b0.
5. Gardner, A. Microscopical Effect of Penicillin on Spores and Vegetative Cells of Bacilli. *Lancet* **1945**, 658–659.
6. Hutchings, M.I.; Truman, A.W.; Wilkinson, B. Antibiotics: past, present and future. *Curr Opin Microbiol* **2019**, *51*, 72–80, doi:10.1016/j.mib.2019.10.008.

7. Walsh, C. Molecular mechanisms that confer antibacterial drug resistance. *Nature* **2000**, *406*, 775–781, doi:10.1038/35021219.
8. Luepke, K.H.; Suda, K.J.; Boucher, H.; Russo, R.L.; Bonney, M.W.; Hunt, T.D.; Mohr, J.F. Past, Present, and Future of Antibacterial Economics: Increasing Bacterial Resistance, Limited Antibiotic Pipeline, and Societal Implications. *Pharmacotherapy* **2017**, *37*, 71–84, doi:10.1002/phar.1868.
9. Tacconelli, E.; Carrara, E.; Savoldi, A.; Harbarth, S.; Mendelson, M.; Monnet, D.L.; Pulcini, C.; Kahlmeter, G.; Kluytmans, J.; Carmeli, Y.; et al. Discovery, research, and development of new antibiotics: the WHO priority list of antibiotic-resistant bacteria and tuberculosis. *The Lancet Infectious Diseases* **2018**, *18*, 318–327, doi:10.1016/S1473-3099(17)30753-3.
10. Zampaloni, C.; Mattei, P.; Bleicher, K.; Winther, L.; Thäte, C.; Bucher, C.; Adam, J.-M.; Alanine, A.; Amrein, K.E.; Baidin, V.; et al. A novel antibiotic class targeting the lipopolysaccharide transporter. *Nature* **2024**, *625*, 566–571, doi:10.1038/s41586-023-06873-0.
11. Quach, D.T.; Sakoulas, G.; Nizet, V.; Pogliano, J.; Pogliano, K. Bacterial Cytological Profiling (BCP) as a Rapid and Accurate Antimicrobial Susceptibility Testing Method for Staphylococcus aureus. *EBioMedicine* **2016**, *4*, 95–103, doi:10.1016/j.ebiom.2016.01.020.
12. Samernate, T.; Htoo, H.H.; Sugie, J.; Chavasiri, W.; Pogliano, J.; Chaikeeratisak, V.; Nonejuie, P. High-Resolution Bacterial Cytological Profiling Reveals Intrapopulation Morphological Variations upon Antibiotic Exposure. *Antimicrob Agents Chemother* **2023**, *67*, e01307-22, doi:10.1128/aac.01307-22.
13. Nonejuie, P.; Burkart, M.; Pogliano, K.; Pogliano, J. Bacterial cytological profiling rapidly identifies the cellular pathways targeted by antibacterial molecules. *Proc. Natl. Acad. Sci. U.S.A.* **2013**, *110*, 16169–16174, doi:10.1073/pnas.1311066110.
14. Deep, A.; Liang, Q.; Enustun, E.; Pogliano, J.; Corbett, K.D. Architecture and activation mechanism of the bacterial PARIS defence system. *Nature* **2024**, 1–8, doi:10.1038/s41586-024-07772-8.
15. Tsunemoto, H.; Sugie, J.; Enustun, E.; Pogliano, K.; Pogliano, J. Bacterial cytological profiling reveals interactions between jumbo phage φKZ infection and cell wall active antibiotics in Pseudomonas aeruginosa. *PloS one* **2023**, *18*, e0280070, doi:10.1371/journal.pone.0280070.
16. Birkholz, E.A.; Morgan, C.J.; Laughlin, T.G.; Lau, R.K.; Prichard, A.; Rangarajan, S.; Meza, G.N.; Lee, J.; Armbruster, E.; Suslov, S.; et al. An intron endonuclease facilitates interference competition between coinfecting viruses. *Science* **2024**, *385*, 105–112, doi:10.1126/science.adl1356.
17. Thammatinna, K.; Egan, M.E.; Htoo, H.H.; Khanna, K.; Sugie, J.; Nideffer, J.F.; Villa, E.; Tassanakajon, A.; Pogliano, J.; Nonejuie, P.; et al. A novel vibriophage exhibits inhibitory activity against host protein synthesis machinery. *Sci Rep* **2020**, *10*, 2347, doi:10.1038/s41598-020-59396-3.
18. Soonthonsrima, T.; Htoo, H.H.; Thiennimitr, P.; Srisuknimit, V.; Nonejuie, P.; Chaikeeratisak, V. Phage-induced bacterial morphological changes reveal a phage-derived antimicrobial affecting cell wall integrity. *Antimicrobial Agents and Chemotherapy* **2023**, *67*, e00764-23, doi:10.1128/aac.00764-23.
19. Naknaen, A.; Samernate, T.; Wannasrichan, W.; Surachat, K.; Nonejuie, P.; Chaikeeratisak, V. Combination of genetically diverse Pseudomonas phages enhances the cocktail efficiency against bacteria. *Sci Rep* **2023**, *13*, 8921, doi:10.1038/s41598-023-36034-2.
20. Naknaen, A.; Samernate, T.; Saeju, P.; Nonejuie, P.; Chaikeeratisak, V. Nucleus-forming jumbophage PhiKZ therapeutically outcompetes non-nucleus-forming jumbophage Callisto. *iScience* **2024**, *27*, 109790, doi:10.1016/j.isci.2024.109790.
21. Corona, F.; Martinez, J.L. Phenotypic Resistance to Antibiotics. *Antibiotics* **2013**, *2*, 237–255, doi:10.3390/antibiotics2020237.
22. Davies, J.; Davies, D. Origins and Evolution of Antibiotic Resistance. *Microbiology and Molecular Biology Reviews* **2010**, *74*, 417–433, doi:10.1128/mmbr.00016-10.
23. Cotsonas King, A.; Wu, L. Macromolecular Synthesis and Membrane Perturbation Assays for Mechanisms of Action Studies of Antimicrobial Agents. *CP Pharmacology* **2009**, *47*, doi:10.1002/0471141755.ph13a07s47.
24. Lima, L.M.; Silva, B.N.M. da; Barbosa, G.; Barreiro, E.J. β-lactam antibiotics: An overview from a medicinal chemistry perspective. *Eur J Med Chem* **2020**, *208*, 112829, doi:10.1016/j.ejmech.2020.112829.
25. Baquero, F.; Levin, B.R. Proximate and ultimate causes of the bactericidal action of antibiotics. *Nat Rev Microbiol* **2021**, *19*, 123–132, doi:10.1038/s41579-020-00443-1.
26. Reynolds, P.E. Structure, biochemistry and mechanism of action of glycopeptide antibiotics. *Eur. J. Clin. Microbiol. Infect. Dis.* **1989**, *8*, 943–950, doi:10.1007/BF01967563.
27. Jerala, R. Synthetic lipopeptides: a novel class of anti-infectives. *Expert Opin Investig Drugs* **2007**, *16*, 1159–1169, doi:10.1517/13543784.16.8.1159.
28. O'Rourke, A.; Beyhan, S.; Choi, Y.; Morales, P.; Chan, A.P.; Espinoza, J.L.; Dupont, C.L.; Meyer, K.J.; Spoering, A.; Lewis, K.; et al. Mechanism-of-Action Classification of Antibiotics by Global Transcriptome Profiling. *Antimicrob Agents Chemother* **2020**, *64*, e01207-19, doi:10.1128/AAC.01207-19.
29. PubChem Cerulenin Available online: https://pubchem.ncbi.nlm.nih.gov/compound/5282054 (accessed on Aug 14, 2024).

30. Davis, B.D.; Chen, L.L.; Tai, P.C. Misread protein creates membrane channels: an essential step in the bactericidal action of aminoglycosides. *Proc Natl Acad Sci U S A* **1986**, *83*, 6164–6168, doi:10.1073/pnas.83.16.6164.
31. Chopra, I.; Roberts, M. Tetracycline Antibiotics: Mode of Action, Applications, Molecular Biology, and Epidemiology of Bacterial Resistance. *Microbiol Mol Biol Rev* **2001**, *65*, 232–260, doi:10.1128/MMBR.65.2.232-260.2001.
32. Vázquez-Laslop, N.; Mankin, A.S. How Macrolide Antibiotics Work. *Trends Biochem Sci* **2018**, *43*, 668–684, doi:10.1016/j.tibs.2018.06.011.
33. Tenson, T.; Lovmar, M.; Ehrenberg, M. The Mechanism of Action of Macrolides, Lincosamides and Streptogramin B Reveals the Nascent Peptide Exit Path in the Ribosome. *Journal of Molecular Biology* **2003**, *330*, 1005–1014, doi:10.1016/S0022-2836(03)00662-4.
34. Swaney, S.M.; Aoki, H.; Ganoza, M.C.; Shinabarger, D.L. The oxazolidinone linezolid inhibits initiation of protein synthesis in bacteria. *Antimicrob Agents Chemother* **1998**, *42*, 3251–3255, doi:10.1128/AAC.42.12.3251.
35. Correia, S.; Poeta, P.; Hébraud, M.; Capelo, J.L.; Igrejas, G. Mechanisms of quinolone action and resistance: where do we stand? *J Med Microbiol* **2017**, *66*, 551–559, doi:10.1099/jmm.0.000475.
36. Ojkic, N.; Lilja, E.; Direito, S.; Dawson, A.; Allen, R.J.; Waclaw, B. A Roadblock-and-Kill Mechanism of Action Model for the DNA-Targeting Antibiotic Ciprofloxacin. *Antimicrob Agents Chemother* **2020**, *64*, e02487-19, doi:10.1128/AAC.02487-19.
37. Wong, W.R.; Oliver, A.G.; Linington, R.G. Development of Antibiotic Activity Profile Screening for the Classification and Discovery of Natural Product Antibiotics. *Chemistry & Biology* **2012**, *19*, 1483–1495, doi:10.1016/j.chembiol.2012.09.014.
38. Kohanski, M.A.; Dwyer, D.J.; Collins, J.J. How antibiotics kill bacteria: from targets to networks. *Nat Rev Microbiol* **2010**, *8*, 423–435, doi:10.1038/nrmicro2333.
39. WHO AWaRe classification of antibiotics for evaluation and monitoring of use, 2023 2023.
40. Silver, L.L. Challenges of Antibacterial Discovery. *Clin Microbiol Rev* **2011**, *24*, 71–109, doi:10.1128/CMR.00030-10.
41. Hudson, M.A.; Lockless, S.W. Elucidating the Mechanisms of Action of Antimicrobial Agents. *mBio 13*, e02240-21, doi:10.1128/mbio.02240-21.
42. Hage, D.S.; Anguizola, J.A.; Bi, C.; Li, R.; Matsuda, R.; Papastavros, E.; Pfaunmiller, E.; Vargas, J.; Zheng, X. Pharmaceutical and biomedical applications of affinity chromatography: Recent trends and developments. *Journal of Pharmaceutical and Biomedical Analysis* **2012**, *69*, 93–105, doi:10.1016/j.jpba.2012.01.004.
43. Franken, H.; Mathieson, T.; Childs, D.; Sweetman, G.M.A.; Werner, T.; Tögel, I.; Doce, C.; Gade, S.; Bantscheff, M.; Drewes, G.; et al. Thermal proteome profiling for unbiased identification of direct and indirect drug targets using multiplexed quantitative mass spectrometry. *Nat Protoc* **2015**, *10*, 1567–1593, doi:10.1038/nprot.2015.101.
44. Lewis, K. Platforms for antibiotic discovery. *Nat Rev Drug Discov* **2013**, *12*, 371–387, doi:10.1038/nrd3975.
45. Lewis, K.; Lee, R.E.; Brötz-Oesterhelt, H.; Hiller, S.; Rodnina, M.V.; Schneider, T.; Weingarth, M.; Wohlgemuth, I. Sophisticated natural products as antibiotics. *Nature* **2024**, *632*, 39–49, doi:10.1038/s41586-024-07530-w.
46. Balaban, N.Q.; Helaine, S.; Lewis, K.; Ackermann, M.; Aldridge, B.; Andersson, D.I.; Brynildsen, M.P.; Bumann, D.; Camilli, A.; Collins, J.J.; et al. Definitions and guidelines for research on antibiotic persistence. *Nat Rev Microbiol* **2019**, *17*, 441–448, doi:10.1038/s41579-019-0196-3.
47. Kussell, E.; Kishony, R.; Balaban, N.Q.; Leibler, S. Bacterial Persistence. *Genetics* **2005**, *169*, 1807–1814, doi:10.1534/genetics.104.035352.
48. Bailey, S. Principal Component Analysis with Noisy and/or Missing Data. *Publications of the Astronomical Society of the Pacific* **2012**, *124*, 1015–1023, doi:10.1086/668105.
49. Van Den Broeck, T.; Joniau, S.; Clinckemalie, L.; Helsen, C.; Prekovic, S.; Spans, L.; Tosco, L.; Van Poppel, H.; Claessens, F. The Role of Single Nucleotide Polymorphisms in Predicting Prostate Cancer Risk and Therapeutic Decision Making. *BioMed Research International* **2014**, *2014*, 1–16, doi:10.1155/2014/627510.
50. Regev, A.; Teichmann, S.A.; Lander, E.S.; Amit, I.; Benoist, C.; Birney, E.; Bodenmiller, B.; Campbell, P.; Carninci, P.; Clatworthy, M.; et al. The Human Cell Atlas. *eLife* **2017**, *6*, e27041, doi:10.7554/eLife.27041.
51. McInnes, L.; Healy, J.; Melville, J. UMAP: Uniform Manifold Approximation and Projection for Dimension Reduction 2020.
52. Wang, Y.; Huang, H.; Rudin, C.; Shaposhnik, Y. Understanding How Dimension Reduction Tools Work: An Empirical Approach to Deciphering t-SNE, UMAP, TriMAP, and PaCMAP for Data Visualization 2021.
53. Martin, J.K.; Sheehan, J.P.; Bratton, B.P.; Moore, G.M.; Mateus, A.; Li, S.H.-J.; Kim, H.; Rabinowitz, J.D.; Typas, A.; Savitski, M.M.; et al. A Dual-Mechanism Antibiotic Kills Gram-Negative Bacteria and Avoids Drug Resistance. *Cell* **2020**, *181*, 1518-1532.e14, doi:10.1016/j.cell.2020.05.005.
54. Takebayashi, Y.; Ramos-Soriano, J.; Jiang, Y.J.; Samphire, J.; Belmonte-Reche, E.; O'Hagan, M.P.; Gurr, C.; Heesom, K.J.; Lewis, P.A.; Samernate, T.; et al. Small molecule G-quadruplex ligands are antibacterial candidates for Gram-negative bacteria 2024, 2022.09.01.506212, doi:10.1101/2022.09.01.506212.

55. Wu, F.; Japaridze, A.; Zheng, X.; Wiktor, J.; Kerssemakers, J.W.J.; Dekker, C. Direct imaging of the circular chromosome in a live bacterium. *Nat Commun* **2019**, *10*, 2194, doi:10.1038/s41467-019-10221-0.
56. Spratt, B.G. Distinct penicillin binding proteins involved in the division, elongation, and shape of Escherichia coli K12. *Proc Natl Acad Sci U S A* **1975**, *72*, 2999–3003.
57. Spratt, B.G.; Pardee, A.B. Penicillin-binding proteins and cell shape in E. coli. *Nature* **1975**, *254*, 516–517, doi:10.1038/254516a0.
58. Curtis, N.A.; Orr, D.; Ross, G.W.; Boulton, M.G. Affinities of penicillins and cephalosporins for the penicillin-binding proteins of Escherichia coli K-12 and their antibacterial activity. *Antimicrob Agents Chemother* **1979**, *16*, 533–539.
59. Di Modugno, E.; Erbetti, I.; Ferrari, L.; Galassi, G.; Hammond, S.M.; Xerri, L. In vitro activity of the tribactam GV104326 against gram-positive, gram-negative, and anaerobic bacteria. *Antimicrob Agents Chemother* **1994**, *38*, 2362–2368.
60. Bernabeu-Wittel, M.; García-Curiel, A.; Pichardo, C.; Pachón-Ibáñez, M.E.; Jiménez-Mejías, M.E.; Pachón, J. Morphological changes induced by imipenem and meropenem at sub-inhibitory concentrations in Acinetobacter baumannii. *Clin Microbiol Infect* **2004**, *10*, 931–934, doi:10.1111/j.1469-0691.2004.00944.x.
61. Jackson, J.J.; Kropp, H. Differences in mode of action of (β-lactam antibiotics influence morphology, LPS release and in vivo antibiotic efficacy. *Journal of Endotoxin Research* **1996**, *3*, 201–218, doi:10.1177/096805199600300306.
62. de Pedro, M.A.; Donachie, W.D.; Höltje, J.-V.; Schwarz, H. Constitutive Septal Murein Synthesis in Escherichia coli with Impaired Activity of the Morphogenetic Proteins RodA and Penicillin-Binding Protein 2. *J Bacteriol* **2001**, *183*, 4115–4126, doi:10.1128/JB.183.14.4115-4126.2001.
63. Sumita, Y.; Fukasawa, M.; Okuda, T. Comparison of two carbapenems, SM-7338 and imipenem: affinities for penicillin-binding proteins and morphological changes. *J Antibiot (Tokyo)* **1990**, *43*, 314–320, doi:10.7164/antibiotics.43.314.
64. Dalhoff, A.; Nasu, T.; Okamoto, K. Target affinities of faropenem to and its impact on the morphology of gram-positive and gram-negative bacteria. *Chemotherapy* **2003**, *49*, 172–183, doi:10.1159/000071141.
65. Horii, T.; Kobayashi, M.; Sato, K.; Ichiyama, S.; Ohta, M. An in-vitro study of carbapenem-induced morphological changes and endotoxin release in clinical isolates of gram-negative bacilli. *J Antimicrob Chemother* **1998**, *41*, 435–442, doi:10.1093/jac/41.4.435.
66. Perumalsamy, H.; Jung, M.Y.; Hong, S.M.; Ahn, Y.-J. Growth-Inhibiting and morphostructural effects of constituents identified in Asarum heterotropoides root on human intestinal bacteria. *BMC Complement Altern Med* **2013**, *13*, 245, doi:10.1186/1472-6882-13-245.
67. Nickerson, W.J.; Webb, M. Effect of folic acid analogues on growth and cell division of nonexacting microorganisms. *J Bacteriol* **1956**, *71*, 129–139.
68. Cushnie, T.P.T.; O'Driscoll, N.H.; Lamb, A.J. Morphological and ultrastructural changes in bacterial cells as an indicator of antibacterial mechanism of action. *Cell. Mol. Life Sci.* **2016**, *73*, 4471–4492, doi:10.1007/s00018-016-2302-2.
69. Elliott, T.S.J.; Shelton, A.; Greenwood, D. The response of Escherichia coli to ciprofloxacin and norfloxacin. *Journal of Medical Microbiology* **1987**, *23*, 83–88, doi:10.1099/00222615-23-1-83.
70. Chen, K.; Sun, G.W.; Chua, K.L.; Gan, Y.-H. Modified Virulence of Antibiotic-Induced Burkholderia pseudomallei Filaments. *Antimicrob Agents Chemother* **2005**, *49*, 1002–1009, doi:10.1128/AAC.49.3.1002-1009.2005.
71. Uphoff, S.; Reyes-Lamothe, R.; Garza de Leon, F.; Sherratt, D.J.; Kapanidis, A.N. Single-molecule DNA repair in live bacteria. *Proceedings of the National Academy of Sciences* **2013**, *110*, 8063–8068, doi:10.1073/pnas.1301804110.
72. Jones, E.C.; Uphoff, S. Single-molecule imaging of LexA degradation in Escherichia coli elucidates regulatory mechanisms and heterogeneity of the SOS response. *Nat Microbiol* **2021**, *6*, 981–990, doi:10.1038/s41564-021-00930-y.
73. Jaramillo-Riveri, S.; Broughton, J.; McVey, A.; Pilizota, T.; Scott, M.; El Karoui, M. Growth-dependent heterogeneity in the DNA damage response in Escherichia coli. *Mol Syst Biol* **2022**, *18*, e10441, doi:10.15252/msb.202110441.
74. Gebicki, J.M.; James, A.M. The Preparation and Properties of Spheroplasts of Aerobacter aerogenes. *Journal of General Microbiology* **1960**, *23*, 9–18, doi:10.1099/00221287-23-1-9.
75. Errington, J. L-form bacteria, cell walls and the origins of life. *Open Biol* **2013**, *3*, 120143, doi:10.1098/rsob.120143.
76. Allan, E.J.; Hoischen, C.; Gumpert, J. Bacterial L-forms. *Adv Appl Microbiol* **2009**, *68*, 1–39, doi:10.1016/S0065-2164(09)01201-5.
77. Mercier, R.; Kawai, Y.; Errington, J. General principles for the formation and proliferation of a wall-free (L-form) state in bacteria. *eLife* **2014**, *3*, e04629, doi:10.7554/eLife.04629.
78. Errington, J. Cell wall-deficient, L-form bacteria in the 21st century: a personal perspective. *Biochem Soc Trans* **2017**, *45*, 287–295, doi:10.1042/BST20160435.

79. Banerjee, S.; Lo, K.; Ojkic, N.; Stephens, R.; Scherer, N.F.; Dinner, A.R. Mechanical feedback promotes bacterial adaptation to antibiotics. *Nat. Phys.* **2021**, *17*, 403–409, doi:10.1038/s41567-020-01079-x.
80. Ojkic, N.; Serbanescu, D.; Banerjee, S. Antibiotic Resistance via Bacterial Cell Shape-Shifting. *mBio* **2022**, *13*, e00659-22, doi:10.1128/mbio.00659-22.
81. Ojkic, N.; Serbanescu, D.; Banerjee, S. Surface-to-volume scaling and aspect ratio preservation in rod-shaped bacteria. *eLife* **2019**, *8*, e47033, doi:10.7554/eLife.47033.
82. Ojkic, N.; Banerjee, S. Bacterial cell shape control by nutrient-dependent synthesis of cell division inhibitors. *Biophysical Journal* **2021**, *120*, 2079–2084, doi:10.1016/j.bpj.2021.04.001.
83. Lin, L.; Nonejuie, P.; Munguia, J.; Hollands, A.; Olson, J.; Dam, Q.; Kumaraswamy, M.; Rivera, H.; Corriden, R.; Rohde, M.; et al. Azithromycin Synergizes with Cationic Antimicrobial Peptides to Exert Bactericidal and Therapeutic Activity Against Highly Multidrug-Resistant Gram-Negative Bacterial Pathogens. *EBioMedicine* **2015**, *2*, 690–698, doi:10.1016/j.ebiom.2015.05.021.
84. Mohammad, H.; Younis, W.; Ezzat, H.G.; Peters, C.E.; AbdelKhalek, A.; Cooper, B.; Pogliano, K.; Pogliano, J.; Mayhoub, A.S.; Seleem, M.N. Bacteriological profiling of diphenylureas as a novel class of antibiotics against methicillin-resistant Staphylococcus aureus. *PLoS ONE* **2017**, *12*, e0182821, doi:10.1371/journal.pone.0182821.
85. Wu, Y.; Seyedsayamdost, M.R. The Polyene Natural Product Thailandamide A Inhibits Fatty Acid Biosynthesis in Gram-Positive and Gram-Negative Bacteria. *Biochemistry* **2018**, *57*, 4247–4251, doi:10.1021/acs.biochem.8b00678.
86. Sun, Y.; Heidary, D.K.; Zhang, Z.; Richards, C.I.; Glazer, E.C. Bacterial Cytological Profiling Reveals the Mechanism of Action of Anticancer Metal Complexes. *Mol. Pharmaceutics* **2018**, *15*, 3404–3416, doi:10.1021/acs.molpharmaceut.8b00407.
87. Dillon, N.A.; Seif, Y.; Tsunemoto, H.; Poudel, S.; Meehan, M.; Szubin, R.; Olson, C.; Rajput, A.; Alarcon, G.; Lamsa, A.; et al. Characterizing the response of *Acinetobacter baumannii* ATCC 17978 to azithromycin in multiple *in vitro* growth conditions 2020, doi:10.1101/2020.05.19.079962.
88. Araújo-Bazán, L.; Ruiz-Avila, L.B.; Andreu, D.; Huecas, S.; Andreu, J.M. Cytological Profile of Antibacterial FtsZ Inhibitors and Synthetic Peptide MciZ. *Front. Microbiol.* **2016**, *7*, doi:10.3389/fmicb.2016.01558.
89. Andreu, J.M.; Huecas, S.; Araújo-Bazán, L.; Vázquez-Villa, H.; Martín-Fontecha, M. The Search for Antibacterial Inhibitors Targeting Cell Division Protein FtsZ at Its Nucleotide and Allosteric Binding Sites. *Biomedicines* **2022**, *10*, 1825, doi:10.3390/biomedicines10081825.
90. World Healt Organization WHO Bacterial Priority Pathogens List, 2017 2017.
91. Di Bella, S.; Giacobbe, D.R.; Maraolo, A.E.; Viaggi, V.; Luzzati, R.; Bassetti, M.; Luzzaro, F.; Principe, L. Resistance to ceftazidime/avibactam in infections and colonisations by KPC-producing Enterobacterales: a systematic review of observational clinical studies. *Journal of Global Antimicrobial Resistance* **2021**, *25*, 268–281, doi:10.1016/j.jgar.2021.04.001.
92. Butler, M.S.; Gigante, V.; Sati, H.; Paulin, S.; Al-Sulaiman, L.; Rex, J.H.; Fernandes, P.; Arias, C.A.; Paul, M.; Thwaites, G.E.; et al. Analysis of the Clinical Pipeline of Treatments for Drug-Resistant Bacterial Infections: Despite Progress, More Action Is Needed. *Antimicrob Agents Chemother 66*, e01991-21, doi:10.1128/aac.01991-21.
93. Geneva: World Health Organization WHO Bacterial Priority Pathogens List, 2024: bacterial pathogens of public health importance to guide research, development and strategies to prevent and control antimicrobial resistance. 2024.
94. Htoo, H.H.; Brumage, L.; Chaikeeratisak, V.; Tsunemoto, H.; Sugie, J.; Tribuddharat, C.; Pogliano, J.; Nonejuie, P. Bacterial Cytological Profiling as a Tool To Study Mechanisms of Action of Antibiotics That Are Active against Acinetobacter baumannii. *Antimicrobial Agents and Chemotherapy* **2019**, *63*, 10.1128/aac.02310-18, doi:10.1128/aac.02310-18.
95. Coram, M.A.; Wang, L.; Godinez, W.J.; Barkan, D.T.; Armstrong, Z.; Ando, D.M.; Feng, B.Y. Morphological Characterization of Antibiotic Combinations. *ACS Infect. Dis.* **2022**, *8*, 66–77, doi:10.1021/acsinfecdis.1c00312.
96. Montaño, E.T.; Nideffer, J.F.; Sugie, J.; Enustun, E.; Shapiro, A.B.; Tsunemoto, H.; Derman, A.I.; Pogliano, K.; Pogliano, J. Bacterial Cytological Profiling Identifies Rhodanine-Containing PAINS Analogs as Specific Inhibitors of Escherichia coli Thymidylate Kinase In Vivo. *Journal of Bacteriology* **2021**, *203*, 10.1128/jb.00105-21, doi:10.1128/jb.00105-21.
97. Nonejuie, P.; Trial, R.M.; Newton, G.L.; Lamsa, A.; Ranmali Perera, V.; Aguilar, J.; Liu, W.-T.; Dorrestein, P.C.; Pogliano, J.; Pogliano, K. Application of bacterial cytological profiling to crude natural product extracts reveals the antibacterial arsenal of Bacillus subtilis. *J Antibiot* **2016**, *69*, 353–361, doi:10.1038/ja.2015.116.
98. Sun, D.; Tsivkovski, R.; Pogliano, J.; Tsunemoto, H.; Nelson, K.; Rubio-Aparicio, D.; Lomovskaya, O. Intrinsic Antibacterial Activity of Xeruborbactam In Vitro: Assessing Spectrum and Mode of Action. *Antimicrob Agents Chemother 66*, e00879-22, doi:10.1128/aac.00879-22.

99. Sridhar, S.; Forrest, S.; Warne, B.; Maes, M.; Baker, S.; Dougan, G.; Bartholdson Scott, J. High-Content Imaging to Phenotype Antimicrobial Effects on Individual Bacteria at Scale. *mSystems 6*, e00028-21, doi:10.1128/mSystems.00028-21.
100. Smith, T.C.; Pullen, K.M.; Olson, M.C.; McNellis, M.E.; Richardson, I.; Hu, S.; Larkins-Ford, J.; Wang, X.; Freundlich, J.S.; Ando, D.M.; et al. Morphological profiling of tubercle bacilli identifies drug pathways of action. *Proc Natl Acad Sci U S A* **2020**, *117*, 18744–18753, doi:10.1073/pnas.2002738117.
101. Allen, R.; Ames, L.; Baldin, V.P.; Butts, A.; Henry, K.J.; Quach, D.; Sugie, J.; Pogliano, J.; Parish, T. An arylsulphonamide that targets cell wall biosynthesis in Mycobacterium tuberculosis 2024, 2024.07.22.604653, doi:10.1101/2024.07.22.604653.
102. López-Jiménez, A.T.; Brokatzky, D.; Pillay, K.; Williams, T.; Güler, G.Ö.; Mostowy, S. High-content high-resolution microscopy and deep learning assisted analysis reveals host and bacterial heterogeneity during Shigella infection. *eLife* **2024**, *13*, doi:10.7554/eLife.97495.1.
103. Werth, B.J.; Steed, M.E.; Ireland, C.E.; Tran, T.T.; Nonejuie, P.; Murray, B.E.; Rose, W.E.; Sakoulas, G.; Pogliano, J.; Arias, C.A.; et al. Defining Daptomycin Resistance Prevention Exposures in Vancomycin-Resistant Enterococcus faecium and E. faecalis. *Antimicrob Agents Chemother* **2014**, *58*, 5253–5261, doi:10.1128/AAC.00098-14.
104. Kalla, G. Using Bacterial Cytological Profiling to Study the Interactions of Bacteria and the Defense Systems of Multicellular Eukaryotes, University of California San Diego: USA, 2020.
105. Blaskovich, M.A.T.; Kavanagh, A.M.; Elliott, A.G.; Zhang, B.; Ramu, S.; Amado, M.; Lowe, G.J.; Hinton, A.O.; Pham, D.M.T.; Zuegg, J.; et al. The antimicrobial potential of cannabidiol. *Commun Biol* **2021**, *4*, 1–18, doi:10.1038/s42003-020-01530-y.
106. Sakoulas, G.; Nonejuie, P.; Kullar, R.; Pogliano, J.; Rybak, M.J.; Nizet, V. Examining the Use of Ceftaroline in the Treatment of Streptococcus pneumoniae Meningitis with Reference to Human Cathelicidin LL-37. *Antimicrob Agents Chemother* **2015**, *59*, 2428–2431, doi:10.1128/AAC.04965-14.
107. Schäfer, A.-B.; Sidarta, M.; Abdelmesseh Nekhala, I.; Marinho Righetto, G.; Arshad, A.; Wenzel, M. Dissecting antibiotic effects on the cell envelope using bacterial cytological profiling: a phenotypic analysis starter kit. *Microbiol Spectr* **2024**, *12*, e03275-23, doi:10.1128/spectrum.03275-23.
108. Serbanescu, D.; Ojkic, N.; Banerjee, S. Cellular resource allocation strategies for cell size and shape control in bacteria. *The FEBS Journal* **2022**, *289*, 7891–7906, doi:10.1111/febs.16234.
109. McQuin, C.; Goodman, A.; Chernyshev, V.; Kamentsky, L.; Cimini, B.A.; Karhohs, K.W.; Doan, M.; Ding, L.; Rafelski, S.M.; Thirstrup, D.; et al. CellProfiler 3.0: Next-generation image processing for biology. *PLOS Biology* **2018**, *16*, e2005970, doi:10.1371/journal.pbio.2005970.
110. Berg, S.; Kutra, D.; Kroeger, T.; Straehle, C.N.; Kausler, B.X.; Haubold, C.; Schiegg, M.; Ales, J.; Beier, T.; Rudy, M.; et al. ilastik: interactive machine learning for (bio)image analysis. *Nat Methods* **2019**, *16*, 1226–1232, doi:10.1038/s41592-019-0582-9.
111. Schindelin, J.; Arganda-Carreras, I.; Frise, E.; Kaynig, V.; Longair, M.; Pietzsch, T.; Preibisch, S.; Rueden, C.; Saalfeld, S.; Schmid, B.; et al. Fiji: an open-source platform for biological-image analysis. *Nat Methods* **2012**, *9*, 676–682, doi:10.1038/nmeth.2019.
112. Korsunsky, I.; Millard, N.; Fan, J.; Slowikowski, K.; Zhang, F.; Wei, K.; Baglaenko, Y.; Brenner, M.; Loh, P.; Raychaudhuri, S. Fast, sensitive and accurate integration of single-cell data with Harmony. *Nat Methods* **2019**, *16*, 1289–1296, doi:10.1038/s41592-019-0619-0.
113. Lamsa, A.; Lopez-Garrido, J.; Quach, D.; Riley, E.P.; Pogliano, J.; Pogliano, K. Rapid Inhibition Profiling in Bacillus subtilis to Identify the Mechanism of Action of New Antimicrobials. *ACS Chem. Biol.* **2016**, *11*, 2222–2231, doi:10.1021/acschembio.5b01050.
114. Herschede, S.R.; Salam, R.; Gneid, H.; Busschaert, N. Bacterial cytological profiling identifies transmembrane anion transport as the mechanism of action for a urea-based antibiotic. *Supramolecular Chemistry* **2022**, *34*, 26–33, doi:10.1080/10610278.2023.2178921.
115. Ducret, A.; Quardokus, E.M.; Brun, Y.V. MicrobeJ, a tool for high throughput bacterial cell detection and quantitative analysis. *Nat Microbiol* **2016**, *1*, 16077, doi:10.1038/nmicrobiol.2016.77.
116. Montaño, E.T.; Nideffer, J.F.; Sugie, J.; Enustun, E.; Shapiro, A.B.; Tsunemoto, H.; Derman, A.I.; Pogliano, K.; Pogliano, J. Bacterial Cytological Profiling Identifies Rhodanine-Containing PAINS Analogs as Specific Inhibitors of Escherichia coli Thymidylate Kinase In Vivo. *Journal of Bacteriology* **2021**, *203*, 10.1128/jb.00105-21, doi:10.1128/jb.00105-21.
117. Hausen, R.; Robertson, B.E. Morpheus: A Deep Learning Framework for the Pixel-level Analysis of Astronomical Image Data. *ApJS* **2020**, *248*, 20, doi:10.3847/1538-4365/ab8868.
118. Paintdakhi, A.; Parry, B.; Campos, M.; Irnov, I.; Elf, J.; Surovtsev, I.; Jacobs-Wagner, C. Oufti: An integrated software package for high-accuracy, high-throughput quantitative microscopy analysis. *Mol Microbiol* **2016**, *99*, 767–777, doi:10.1111/mmi.13264.
119. Santos, T.M.A.; Lammers, M.G.; Zhou, M.; Sparks, I.L.; Rajendran, M.; Fang, D.; De Jesus, C.L.Y.; Carneiro, G.F.R.; Cui, Q.; Weibel, D.B. Small Molecule Chelators Reveal That Iron Starvation Inhibits Late Stages of Bacterial Cytokinesis. *ACS Chem Biol* **2018**, *13*, 235–246, doi:10.1021/acschembio.7b00560.

120. Ulloa, E.R.; Kousha, A.; Tsunemoto, H.; Pogliano, J.; Licitra, C.; LiPuma, J.J.; Sakoulas, G.; Nizet, V.; Kumaraswamy, M. Azithromycin Exerts Bactericidal Activity and Enhances Innate Immune Mediated Killing of MDR Achromobacter xylosoxidans. *Infectious Microbes & Diseases* **2020**, *2*, 10, doi:10.1097/IM9.0000000000000014.
121. de Wet, T.J.; Winkler, K.R.; Mhlanga, M.; Mizrahi, V.; Warner, D.F. Arrayed CRISPRi and quantitative imaging describe the morphotypic landscape of essential mycobacterial genes. *eLife* **2020**, *9*, e60083, doi:10.7554/eLife.60083.
122. Mayer, B.; Schwan, M.; Thormann, K.M.; Graumann, P.L. Antibiotic Drug screening and Image Characterization Toolbox (A.D.I.C.T.): a robust imaging workflow to monitor antibiotic stress response in bacterial cells in vivo. *F1000Res* **2022**, *10*, 277, doi:10.12688/f1000research.51868.3.
123. Ouyang, X.; Hoeksma, J.; Lubbers, R.J.M.; Siersma, T.K.; Hamoen, L.W.; den Hertog, J. Classification of antimicrobial mechanism of action using dynamic bacterial morphology imaging. *Sci Rep* **2022**, *12*, 11162, doi:10.1038/s41598-022-15405-1.
124. Cutler, K.J.; Stringer, C.; Lo, T.W.; Rappez, L.; Stroustrup, N.; Brook Peterson, S.; Wiggins, P.A.; Mougous, J.D. Omnipose: a high-precision morphology-independent solution for bacterial cell segmentation. *Nat Methods* **2022**, *19*, 1438–1448, doi:10.1038/s41592-022-01639-4.
125. Mistretta, M.; Cimino, M.; Campagne, P.; Volant, S.; Kornobis, E.; Hebert, O.; Rochais, C.; Dallemagne, P.; Lecoutey, C.; Tisnerat, C.; et al. Dynamic microfluidic single-cell screening identifies pheno-tuning compounds to potentiate tuberculosis therapy. *Nat Commun* **2024**, *15*, 4175, doi:10.1038/s41467-024-48269-2.
126. El-sagheir, A.M.K.; Nekhala, I.A.; El-Gaber, M.K.A.; Aboraia, A.S.; Persson, J.; Schäfer, A.-B.; Wenzel, M.; Omar, F.A. Rational design, synthesis, molecular modeling, biological activity, and mechanism of action of polypharmacological norfloxacin hydroxamic acid derivatives. *RSC Med. Chem.* **2023**, *14*, 2593–2610, doi:10.1039/D3MD00309D.
127. Weigert, M.; Schmidt, U. Nuclei instance segmentation and classification in histopathology images with StarDist 2022, doi:10.48550/arXiv.2203.02284.
128. Weigert, M.; Schmidt, U.; Boothe, T.; Müller, A.; Dibrov, A.; Jain, A.; Wilhelm, B.; Schmidt, D.; Broaddus, C.; Culley, S.; et al. Content-aware image restoration: pushing the limits of fluorescence microscopy. *Nat Methods* **2018**, *15*, 1090–1097, doi:10.1038/s41592-018-0216-7.
129. Isola, P.; Zhu, J.-Y.; Zhou, T.; Efros, A.A. Image-to-Image Translation with Conditional Adversarial Networks 2018, doi:10.48550/arXiv.1611.07004.
130. Feng, L.; Wu, K.; Pei, Z.; Weng, T.; Han, Q.; Meng, L.; Qian, X.; Xu, H.; Qiu, Z.; Li, Z.; et al. MLU-Net: A Multi-Level Lightweight U-Net for Medical Image Segmentation Integrating Frequency Representation and MLP-Based Methods. *IEEE Access* **2024**, *12*, 20734–20751, doi:10.1109/ACCESS.2024.3360889.
131. Mandal, S.; Uhlmann, V. Splinedist: Automated Cell Segmentation With Spline Curves. In Proceedings of the 2021 IEEE 18th International Symposium on Biomedical Imaging (ISBI); 2021; pp. 1082–1086.
132. Spahn, C.; Gómez-de-Mariscal, E.; Laine, R.F.; Pereira, P.M.; Von Chamier, L.; Conduit, M.; Pinho, M.G.; Jacquemet, G.; Holden, S.; Heilemann, M.; et al. DeepBacs for multi-task bacterial image analysis using open-source deep learning approaches. *Commun Biol* **2022**, *5*, 688, doi:10.1038/s42003-022-03634-z.
133. Kuru, E.; Hughes, H.V.; Brown, P.J.; Hall, E.; Tekkam, S.; Cava, F.; de Pedro, M.A.; Brun, Y.V.; VanNieuwenhze, M.S. In Situ Probing of Newly Synthesized Peptidoglycan in Live Bacteria with Fluorescent D -Amino Acids. *Angew Chem Int Ed* **2012**, *51*, 12519–12523, doi:10.1002/anie.201206749.
134. Vollmer, W.; Blanot, D.; de Pedro, M.A. Peptidoglycan structure and architecture. *FEMS Microbiol Rev* **2008**, *32*, 149–167, doi:10.1111/j.1574-6976.2007.00094.x.
135. Young, K.D. The Selective Value of Bacterial Shape. *Microbiol Mol Biol Rev* **2006**, *70*, 660–703, doi:10.1128/MMBR.00001-06.
136. Stratford, J.P.; Edwards, C.L.A.; Ghanshyam, M.J.; Malyshev, D.; Delise, M.A.; Hayashi, Y.; Asally, M. Electrically induced bacterial membrane-potential dynamics correspond to cellular proliferation capacity. *Proc. Natl. Acad. Sci. U.S.A.* **2019**, *116*, 9552–9557, doi:10.1073/pnas.1901788116.
137. Prindle, A.; Liu, J.; Asally, M.; Ly, S.; Garcia-Ojalvo, J.; Süel, G.M. Ion channels enable electrical communication in bacterial communities. *Nature* **2015**, *527*, 59–63, doi:10.1038/nature15709.
138. De Souza-Guerreiro, T.C.; Huan Bacellar, L.; Da Costa, T.S.; Edwards, C.L.A.; Tasic, L.; Asally, M. Membrane potential dynamics unveil the promise of bioelectrical antimicrobial susceptibility Testing (BeAST) for anti-fungal screening. *mBio* **2024**, *15*, e01302-24, doi:10.1128/mbio.01302-24.
139. Wong, F.; Stokes, J.M.; Cervantes, B.; Penkov, S.; Friedrichs, J.; Renner, L.D.; Collins, J.J. Cytoplasmic condensation induced by membrane damage is associated with antibiotic lethality. *Nat Commun* **2021**, *12*, 2321, doi:10.1038/s41467-021-22485-6.
140. Ma, J.; Xie, R.; Ayyadhury, S.; Ge, C.; Gupta, A.; Gupta, R.; Gu, S.; Zhang, Y.; Lee, G.; Kim, J.; et al. The multimodality cell segmentation challenge: toward universal solutions. *Nat Methods* **2024**, *21*, 1103–1113, doi:10.1038/s41592-024-02233-6.

141. Bali, A.; Singh, S.N. A Review on the Strategies and Techniques of Image Segmentation. In Proceedings of the 2015 Fifth International Conference on Advanced Computing & Communication Technologies; 2015; pp. 113–120.
142. Stringer, C.; Wang, T.; Michaelos, M.; Pachitariu, M. Cellpose: a generalist algorithm for cellular segmentation. *Nature Methods 2020 18:1* **2020**, *18*, 100–106, doi:10.1038/s41592-020-01018-x.
143. StarDist: Application of the deep-learning tool for phase-contrast cell images - 2020 - Wiley Analytical Science Available online: https://analyticalscience.wiley.com/do/10.1002/was.000400090/ (accessed on Aug 1, 2024).
144. THE ANALYSIS OF CELL IMAGES* - Prewitt - 1966 - Annals of the New York Academy of Sciences - Wiley Online Library Available online: https://nyaspubs.onlinelibrary.wiley.com/doi/abs/10.1111/j.1749-6632.1965.tb11715.x (accessed on Aug 1, 2024).
145. Mendelsohn, M.L.; Kolman, W.A.; Perry, B.; Prewitt, J.M.S. Computer Analysis of Cell Images. *Postgraduate Medicine* **1965**, *38*, 567–573, doi:10.1080/00325481.1965.11695692.
146. Stylianidou, S.; Brennan, C.; Nissen, S.B.; Kuwada, N.J.; Wiggins, P.A. SuperSegger: robust image segmentation, analysis and lineage tracking of bacterial cells. *Molecular Microbiology* **2016**, *102*, 690–700, doi:10.1111/mmi.13486.
147. Chai, B.; Efstathiou, C.; Yue, H.; Draviam, V.M. Opportunities and challenges for deep learning in cell dynamics research. *Trends in Cell Biology* **2023**, *0*, doi:10.1016/j.tcb.2023.10.010.
148. Jan, M.; Spangaro, A.; Lenartowicz, M.; Mattiazzi Usaj, M. From pixels to insights: Machine learning and deep learning for bioimage analysis. *BioEssays* **2024**, *46*, 2300114, doi:10.1002/bies.202300114.
149. Osokin, A.; Chessel, A.; Salas, R.E.C.; Vaggi, F. GANs for Biological Image Synthesis. In Proceedings of the 2017 IEEE International Conference on Computer Vision (ICCV); 2017; pp. 2252–2261.
150. Goldsborough, P.; Pawlowski, N.; Caicedo, J.C.; Singh, S.; Carpenter, A.E. CytoGAN: Generative Modeling of Cell Images 2017, 227645, doi:10.1101/227645.
151. Cylke, C.; Si, F.; Banerjee, S. Effects of antibiotics on bacterial cell morphology and their physiological origins. *Biochemical Society Transactions* **2022**, *50*, 1269–1279, doi:10.1042/BST20210894.
152. Chessel, A.; Carazo Salas, R.E. From observing to predicting single-cell structure and function with high-throughput/high-content microscopy. *Essays in Biochemistry* **2019**, *63*, 197–208, doi:10.1042/EBC20180044.
153. Chong, Y.T.; Koh, J.L.Y.; Friesen, H.; Duffy, S.K.; Cox, M.J.; Moses, A.; Moffat, J.; Boone, C.; Andrews, B.J. Yeast Proteome Dynamics from Single Cell Imaging and Automated Analysis. *Cell* **2015**, *161*, 1413–1424, doi:10.1016/j.cell.2015.04.051.
154. McMahon, C.L.; Esqueda, M.; Yu, J.-J.; Wall, G.; Romo, J.A.; Vila, T.; Chaturvedi, A.; Lopez-Ribot, J.L.; Wormley, F.; Hung, C.-Y. Development of an Imaging Flow Cytometry Method for Fungal Cytological Profiling and Its Potential Application in Antifungal Drug Development. *Journal of Fungi* **2023**, *9*, 722, doi:10.3390/jof9070722.
155. McDiarmid, A.H.; Gospodinova, K.O.; Elliott, R.J.R.; Dawson, J.C.; Graham, R.E.; El-Daher, M.-T.; Anderson, S.M.; Glen, S.C.; Glerup, S.; Carragher, N.O.; et al. Morphological profiling in human neural progenitor cells classifies hits in a pilot drug screen for Alzheimer's disease. *Brain Communications* **2024**, *6*, fcae101, doi:10.1093/braincomms/fcae101.
156. Ren, E.; Kim, S.; Mohamad, S.; Huguet, S.; Shi, Y.; Cohen, A.; Piddini, E.; Carazo-Salas, R. *Deep learning-enhanced morphological profiling predicts cell fate dynamics in real-time in hPSCs*; 2021;
157. Perlman, Z.E.; Slack, M.D.; Feng, Y.; Mitchison, T.J.; Wu, L.F.; Altschuler, S.J. Multidimensional Drug Profiling By Automated Microscopy. *Science* **2004**, *306*, 1194–1198, doi:10.1126/science.1100709.